

Thouless Energy across Many-Body Localization Transition in Floquet Systems

Michael Sonner¹, Maksym Serbyn², Zlatko Papić³ and Dmitry A. Abanin¹

¹*Department of Theoretical Physics, University of Geneva,
24 quai Ernest-Ansermet, 1211 Geneva, Switzerland*

²*IST Austria, Am Campus 1, 3400 Klosterneuburg, Austria and*

³*School of Physics and Astronomy, University of Leeds, Leeds LS2 9JT, United Kingdom*

The notion of Thouless energy plays a central role in the theory of Anderson localization. We investigate and compare the scaling of Thouless energy across the many-body localization (MBL) transition in a Floquet model. We use a combination of methods that are reliable on the ergodic side of the transition (e.g., spectral form factor) and methods that work on the MBL side (e.g. typical matrix elements of local operators) to obtain a complete picture of Thouless energy behavior across the transition. On the ergodic side, Thouless energy tends to a value independent of system size, while at the transition it becomes comparable to the level spacing. Different probes yield consistent estimates of Thouless energy in their overlapping regime of applicability, giving the location of the transition point nearly free of finite-size drift. This work establishes a connection between different definitions of Thouless energy in a many-body setting, and yields new insights into the MBL transition in Floquet systems.

Introduction.— Out-of-equilibrium properties of disordered interacting systems have recently attracted much interest. This attention is due to the remarkable fact that such systems may avoid thermalization via the phenomenon of many-body localization (MBL) [1–4]. The characteristic features of MBL, apart from the system’s long-term memory of the initial state, include logarithmic spreading of entanglement [5, 6] and emergent integrability [7, 8], which is stable with respect to finite but sufficiently weak generic local perturbations. The last property implies that MBL systems represent a paradigm of non-thermal phases of matter, which violate the eigenstate thermalization hypothesis [9–11] at a finite energy density above the ground state.

In addition to stability with respect to perturbations of the Hamiltonian, pioneering works [12–17] have demonstrated the existence of MBL in the presence of periodic driving. In these Floquet systems, MBL allows to avoid unbounded heating, thus enabling the existence of new non-equilibrium phases of matter, such as time crystals [18, 19] and anomalous Floquet insulators [20, 21]. These and related phases are actively investigated in current experiments with NV-centers [22, 23], cold atoms [24], and trapped ions [25].

Despite significant recent progress, many open questions remain in the field of MBL, such as the transition between MBL and delocalized (thermalizing) phase. In studies of localization-delocalization transitions in *single-particle* systems [26, 27], a central role is played by the so-called Thouless energy (E_{Th}) [28]. Intuitively, E_{Th} sets the scale at which the system’s energy levels develop random-matrix-like correlations. On the one hand, E_{Th} is directly linked to a physical observable – the system’s conductance, while on the other hand, E_{Th} can be defined and practically computed by the response of energy levels to the twisting of boundary conditions. Linking seemingly unrelated characteristics of the system, E_{Th} underlies the celebrated scaling theory of localization [29].

The central role of E_{Th} in the understanding of single-

particle localization has motivated its recent extensions to many-body systems. In particular, Ref. [30] introduced a probe based on the behavior of typical matrix elements of local operators, while Refs. [31–34] used spectral properties such as fluctuations of level number and spectral form factor to map out E_{Th} as a function of disorder strength. Refs. [35, 36], following the original Thouless idea, investigated the sensitivity of many-body energy levels to boundary conditions. Furthermore, the behavior of the spectral function was used as a yet another probe of E_{Th} [37]. The inverse of E_{Th} , the Thouless time, can be understood as a characteristic time scale of the system’s dynamics [38]. It is worth noting that E_{Th} is also one of the central building blocks of phenomenological renormalization group studies of MBL-thermal transition [39, 40]. Thus, several candidates for the generalization of E_{Th} to disordered interacting systems have been proposed. However, the comparison of different definitions of E_{Th} is currently missing. Moreover, in Hamiltonian systems, the interpretation of E_{Th} behavior is often complicated by pronounced finite-size effects and non-uniform density of states [41].

The goal of this paper is to compare the behavior of different notions of E_{Th} in many-body systems. Following Ref. [15], we study a many-body Floquet model without any conservation laws, which reduces finite-size effects compared to the more often studied Hamiltonian models, such as the disordered XXZ spin chain [42]. An additional advantage of the Floquet model is that the many-body density of states is uniform, thus removing the need for spectral unfolding [43]. In Hamiltonian models of MBL, on the other hand, the density of states varies strongly with energy; in particular, states at the edge of the spectrum are more localized than those in the center, leading to the many-body mobility edge [30, 44, 45].

Below we demonstrate that a number of different definitions of E_{Th} are qualitatively consistent across the MBL transition in the Floquet model defined in Eq. (1) below. At weak disorder we find that E_{Th} is system-

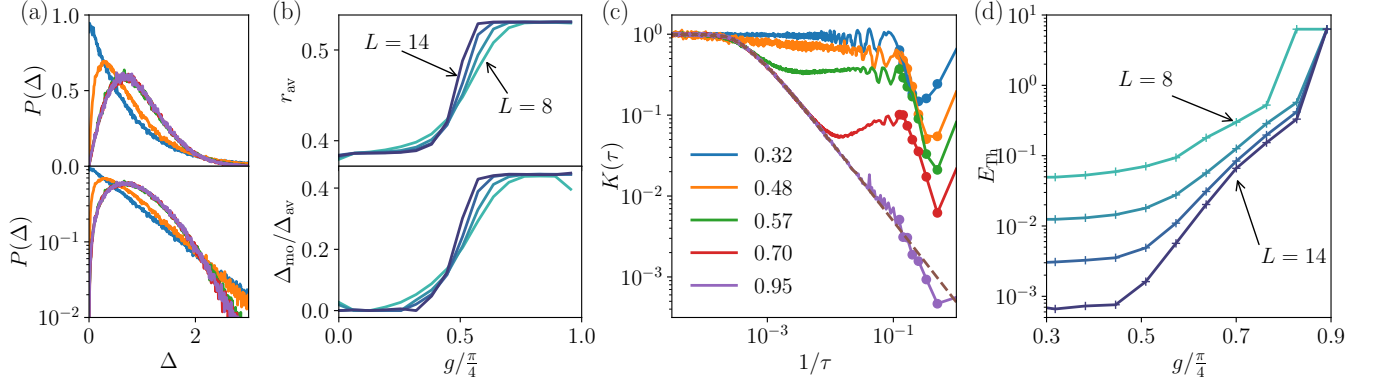


FIG. 1. Spectral properties across the MBL transition. (a) Level spacing distribution for different values of disorder $g/\pi/4$, see legend in panel (c). The curves for the three most ergodic values overlap. (b) Average ratio of adjacent level spacings r_{av} and the most likely level spacing value Δ_* interpolate between different limiting values in the MBL and ergodic phases. Different curves are for system sizes $L = 8, \dots, 14$ and their crossing yields an estimate for the location of MBL transition $g_* \approx 0.36$. (c) Deviation of the spectral form factor $K(\tau)$ from the random matrix prediction (dashed line) occurs at progressively larger values of $1/\tau$ as disorder strength is decreased (g increases). Data shown for $L = 12$ and the values of $g/\pi/4$ are specified in the legend. Dots indicate the data points obtained with exact disorder averaging using a dual transfer matrix approach [46–48]. (d) E_{Th} defined as $1/\tau$ at the point of deviation of $K(\tau)$ from the random matrix curve in panel (c). E_{Th} becomes a constant independent of system size on the ergodic side, while in the transition region E_{Th} decreases exponentially with L .

size independent, consistent with recent analytical results obtained in the large- N limit [32]. E_{Th} decreases upon approaching the MBL transition, becoming smaller than the many-body level spacing. Spectral probes naturally operate in one of the two regimes: (i) the ergodic regime when E_{Th} is large, and (ii) the transition regime and MBL phase, where E_{Th} is comparable to or smaller than level spacing. In contrast, the statistics of matrix elements allows us to access both regimes.

Model.—We consider the following Floquet model for a periodic chain of L spins-1/2, defined by the evolution operator over one driving period:

$$\hat{F} = \exp \left[-i \sum_j g \sigma_j^x \right] \exp \left[-i \sum_j (J \sigma_j^z \sigma_{j+1}^z + h_j \sigma_j^z) \right], \quad (1)$$

where σ_j^α , $\alpha = x, y, z$ are Pauli operators, and $h_j \in [0, 2\pi]$ are uniformly distributed random variables. The parameters g and J determine the importance of disorder in the system. Here, we fix $J = g$ and vary g from 0, where model is trivially localized, to $\pi/4$ where the model (1) becomes “perfectly ergodic” [46, 48, 49], in particular it exactly follows certain predictions of random-matrix theory [48]. Furthermore, Refs. [15, 50] studied a similar Floquet model, with the fields h_j having both a constant and random components; in contrast, in our model h_j are fully random.

In order to study the phase diagram of the model (1) and compare different probes of E_{Th} we use exact diagonalization. We numerically calculate [51] the quasienergies θ_n (defined modulo 2π) and eigenvectors $|n\rangle$ of the Floquet operator, that satisfy $\hat{F}|n\rangle = e^{i\theta_n}|n\rangle$. We first extract E_{Th} from the spectral probes which include level statistics and spectral form factor. Afterwards, we pro-

ceed with the statistics of matrix elements of local operators which allows to extract E_{Th} using typical matrix elements and spectral functions.

Level statistics.—Statistics of (quasi)energy levels has long been used as a probe of quantum chaos and integrability in single-particle systems [52], and in recent years it has been fruitfully applied in a many-body setting. It is worth noting that spectral probes may reveal the breakdown of chaos and ergodicity even when conservation laws are not known explicitly. MBL phase, owing to the emergence of local integrals of motion, exhibits Poisson level statistics, while the ergodic phase is characterized by level repulsion following Wigner-Dyson, random-matrix level statistics [42]. Due to the form of the Floquet operator in Eq. (1), the relevant random matrix theory ensemble is the circular orthogonal ensemble (COE) [43]. These limiting cases of level statistics for the model (1) are demonstrated in Fig. 1(a), which shows the probability distribution of level spacings, $P(\Delta)$, where the level spacing is defined as $\Delta_n = (\theta_{n+1} - \theta_n)/\delta_{av}$, with $\delta_{av} = 2\pi/2^L$. This definition implies that $\langle \Delta \rangle = 1$, and no unfolding is needed due to constant density of states.

At small values of $g \lesssim 0.3$ corresponding to strong disorder, the distribution of level spacings $P(\Delta)$ is Poisson, signalling an MBL phase. At large values of g , when the system is deeply in the ergodic phase, $P(\Delta)$ is described by the COE ensemble. At intermediate values of g , level repulsion is still present, as evidenced by the vanishing of $P(\Delta)$ as $\Delta \rightarrow 0$. However, the maximum Δ_* of $P(\Delta)$ decreases as g is decreased, compared to the random-matrix value. This corresponds to the breakdown of the random-matrix description and weakening of the level repulsion in the critical region, which is also reflected in the softer-than-Gaussian tail of $P(\Delta)$ at large Δ , see bottom

panel of Fig. 1(a).

To estimate the location of MBL-thermal transition from level statistics, we first use the r -parameter [53], defined as $r_{\text{av}} = \langle \min(\Delta_n, \Delta_{n+1}) / \max(\Delta_n, \Delta_{n+1}) \rangle$, where $\langle \dots \rangle$ denotes averaging over the spectrum and different disorder realizations. For the Poisson distribution, this parameter has the value $r_{\text{av}} \approx 0.39$, while for the COE-distributed levels it equals $r_{\text{av}} \approx 0.54$ [54]. The behavior of r_{av} -parameter for different system sizes is illustrated in Fig. 1(b). The curves, interpolating between the Poisson and COE values at small and large g , respectively, cross at $g_* \approx 0.36$, which we take as the location of the critical point separating MBL and thermal phases. We note that the drift of the crossing point with increasing L , which is pronounced in Hamiltonian models, appears to be nearly absent for our model, which we attribute to the absence of conservation laws [15].

An alternative way of estimating the location of the critical point is provided by studying the most likely value of Δ_* , defined by the maximum of $P(\Delta)$. Parameter Δ_* is expected to interpolate between 0 in the MBL phase and a COE value ≈ 0.45 in the ergodic phase. Thus, its finite-size behavior provides a probe of the critical region. Indeed, different curves [Fig. 1(b)] cross at a value consistent with that estimated from r -parameter above.

Spectral form factor.—Spectral form factor (SFF) probes spectral correlations at energy scales larger than the typical level spacing [55]. SFF is given by the Fourier-transform of the two-level correlation function at “time” $\tau > 0$,

$$K(\tau) = \left\langle \left| \text{tr} \left(\hat{F}^\tau \right) \right|^2 \right\rangle = \left\langle \sum_{n,m} e^{i\tau(\theta_n - \theta_m)} \right\rangle, \quad (2)$$

where \hat{F} is the Floquet operator (1), and $\langle \dots \rangle$ denotes disorder averaging. As mentioned above, in our Floquet model there is no need for spectral unfolding, which is necessary for Hamiltonian models. Further, given that quasienergies are defined modulo 2π , we take $\tau \in \mathbb{Z}_+$ taking positive integer values. Qualitatively, SFF at “time” τ probes spectral repulsion, or its absence at the quasienergy scale $\sim 1/\tau$.

Random-matrix theory [43] predicts a linear dependence of SFF on τ . Ergodic systems are expected to exhibit such linear behavior $K(\tau) \propto |\tau|$ at energy scales below E_{Th} , $1/\tau \lesssim E_{\text{Th}}$. Thus, SFF provides a way to extract E_{Th} ; however, this is only possible in the ergodic phase, where E_{Th} is large, while in the MBL phase other means should be sought. We note that at energy scales much smaller than the typical level spacing, $1/\tau \ll \delta_{\text{av}}$, the SFF becomes a constant, irrespective of whether the system is ergodic.

We computed SFF in two complementary ways: first, by directly evaluating Eq. (2) from the energy spectrum and averaging over 100 – 1000 disorder configuration, and, second, using the exactly disorder-averaged dual-transfer matrix approach described in Refs. [46–48]. The

latter method is limited to relatively short times $\tau \sim 10$, but provides a useful benchmark for confirming that the disorder-averaging in the former method is sufficient.

Fig. 1(c) shows that in the ergodic phase ($g \gtrsim g_*$), SFF depends linearly on τ up to $E_{\text{Th}}(g, L)$, as predicted by the random-matrix theory. The scaling of E_{Th} for different system sizes, shown in Fig. 1(d), suggests that in the ergodic phase, $E_{\text{Th}}(g, L) \rightarrow E_{\text{Th}}^*(g)$ as $L \rightarrow \infty$, that is, Thouless energy tends to a constant that does not depend on system size (but depends on g). This is consistent with previous results [32], obtained for a model of q -state spins with $q \rightarrow \infty$ and $d > 1$. In the critical region, we find the scaling $E_{\text{Th}}(g, L) \propto \delta_{\text{av}}$, showing that, similar to Hamiltonian systems, at the MBL-thermal transition the ratio of E_{Th} and level spacing remains approximately constant [30]. Note that the point where E_{Th} extracted from SFF exhibits clear exponential scaling with L coincides with the point where Δ_* remains constant [Fig. 1(b), (d)], demonstrating that the two probes yield consistent results.

Matrix elements.—An attractive feature of spectral probes is their universality: additional conservation laws, irrespective of their precise form, would lead to Poisson level statistics. However, to describe real-time behavior of physical observables, and to obtain insights into the structure of conservation laws in the non-thermalizing phases, it is necessary to study the structure of eigenfunctions and matrix elements of physical operators. Numer-

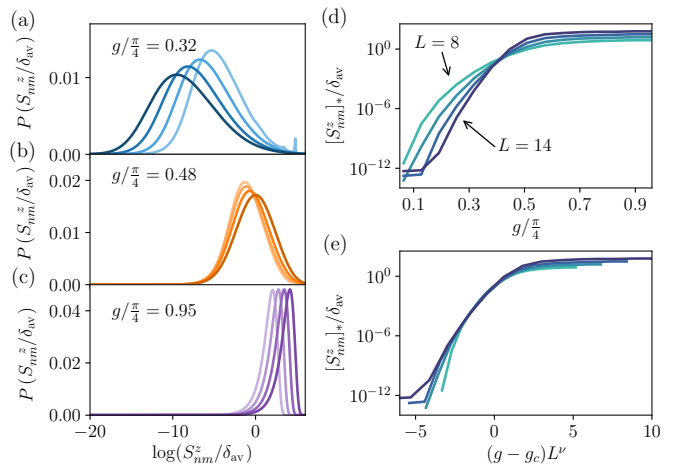


FIG. 2. (a)-(c) Statistics of ratios between matrix elements and level spacing displays qualitatively different behavior in different phases. Color corresponds to system sizes $L = 8, \dots, 14$ in the order of increasing intensity. (a) In the MBL phase the distribution broadens and the typical value decreases exponentially with system size. (b) At the transition, the mode moves very little, but the distribution broadens with L . (c) Deep in the ergodic phase, the evolution of the distribution is consistent with ETH predictions. (d) Mode of the matrix element distribution vs g . The crossing point of curves for different L is consistent with the transition estimate from spectral probes. (e) Scaling collapse of the data in panel (d) gives the critical exponent $\nu \approx 1.2$.

ically, this comes with an added advantage of utilizing more information per sample. Below we will investigate two ways of extracting E_{Th} from matrix elements of local operators, which have been employed in Hamiltonian models of MBL: the ratio between matrix element and level spacing [30] and spectral functions [37, 56].

We first focus on the statistics of matrix elements of a local operator \hat{O} between the Floquet eigenstates, $O_{nm} = |\langle n|\hat{O}|m\rangle|$, and the corresponding “many-body Thouless parameter” defined here as $\mathcal{G} = [O_{nm}/\delta_{\text{av}}]_*$. The notation $[\cdot]_*$ denotes the mode value, this definition is nearly identical to the one that uses an average of the logarithm [30, 51]. Deep in the ergodic phase, matrix elements obey the ETH [9, 10], which implies scaling $O_{nm} \propto \sqrt{\delta_{\text{av}} R_{nm}}$, where R_{nm} are random, normal-distributed numbers with a variance of order one. This corresponds to $\mathcal{G} \propto \delta_{\text{av}}^{-1/2} \gg 1$. In the MBL phase, in contrast, owing to the emergence of local integrals of motion, typical matrix elements decay much faster than the level spacing $\mathcal{G}(L) \propto 2^{-\kappa L}$ with $\kappa > 1$. Further, similar to localized wave functions, the matrix elements develop broad, log-normal distribution [27].

We have studied several local operators for the model (1), and the resulting distribution for the operator $\hat{S}^z = \sigma_1^z/2$ is illustrated in Fig. 2(a)-(c). As expected, we observe that in the MBL phase the distribution $P(S_{nm}^z/\delta_{\text{av}})$ is log-normal, and mode of $S_{nm}^z/\delta_{\text{av}}$ decreases exponentially with L . On the ergodic side, in contrast, this ratio exponentially increases, as predicted by ETH, while the distribution remains narrow. In the critical region, we find that the distribution broadens, while the typical ratio $P(S_{nm}^z/\delta_{\text{av}})$ remains approximately independent of L .

The behavior of \mathcal{G} in Fig. 2(d) serves as an indicator of the location of transition, which yields an estimate consistent with spectral probes. Similar to the finite-size scaling of r_{av} , we do not find any significant drift of the crossing point. An interesting question concerns the relation of \mathcal{G} and Δ_* . We find that on the MBL side of the transition, $\mathcal{G}(L)$ decays much faster compared to the latter quantity. We attribute this to the fact that \mathcal{G} probes matrix elements between eigenstates with quasienergy difference of order one, while Δ_* rather probes matrix elements between nearby energy states, which are enhanced.

In order to obtain the critical exponents, we perform the scaling collapse of $\mathcal{G}(L)$ shown in Fig. 2(e). The value of the critical exponent is $\nu \approx 1.2$, which still violates the Harris criterion [57, 58], however this violation is weaker compared to the exponent in Hamiltonian systems [44]. This, along with the almost absent drift of the crossing point, suggests weaker finite size effects due to the absence of conserved quantities.

Spectral function.—Spectral function (SF) quantifies the energy structure of a matrix element which can be experimentally probed in absorption spectroscopy. SF of an operator \hat{O} is defined as

$$f^2(\omega) = 2^{-L} \sum_{n,m} |\langle n|\hat{O}|m\rangle|^2 \delta(\omega - \theta_n + \theta_m), \quad (3)$$

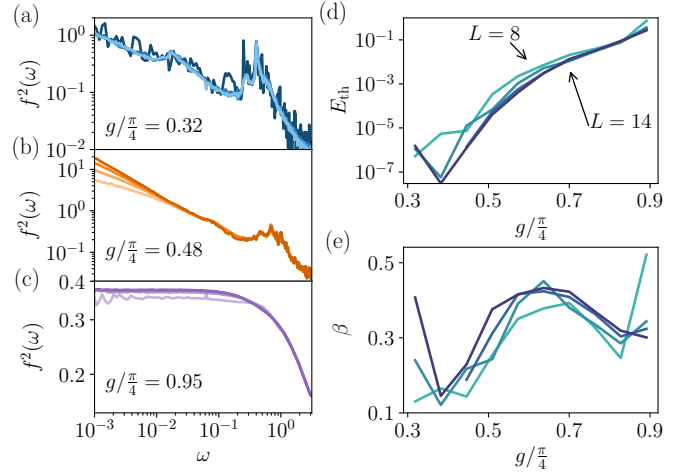


FIG. 3. Spectral function (3) for different system sizes in the MBL phase (a), at the transition (b), and in the fully ergodic phase (c). For energies larger than E_{Th} the spectral function does not depend on system size. Since E_{Th} is very small on the MBL side and constant in the ergodic phase, the spectral function collapses in the full range of considered frequencies. (d) Scaling of E_{Th} extracted from the kww fit to the spectral function [51]. (e) Exponent of the asymptotic power law of the kww fit [59].

where the sum runs over all eigenstates, corresponding to the infinite temperature ensemble. This SF is a Fourier transform of the infinite-temperature real-time correlation function $\langle \hat{O}(t)\hat{O}(0) \rangle_{T=\infty}$, thus, it contains information about the system’s dynamical time scales. In particular, in the ergodic phase, the spectral function has a plateau for $\omega \lesssim E_{\text{Th}}$, since the Thouless time is a scale at which the excitations have propagated through the system and the dynamics have saturated.

The evolution of disorder-averaged spectral function of \hat{S}^z operator, $f^2(\omega)$, across the MBL-thermal transition is illustrated in Fig. 3(a)-(c). Deep in the MBL phase, spectral function develops a delta-function peak at $\omega = 0$ [51], while its behavior at $\omega > 0$ approximately follows power-law behavior, also observed in Hamiltonian MBL systems [37]. In the critical region, a power-law with a larger exponent gradually develops, and spectral function does not exhibit a visible plateau, consistent with E_{Th} becoming of order of the level spacing. Deep in the ergodic phase (c), in contrast, the spectral function is nearly independent of system size, showing a wide plateau, which yields an estimate of E_{Th} consistent with spectral probes.

To quantify E_{Th} from the spectral function we fit $f^2(\omega)$ using the Fourier transform of a stretched exponential (so-called kww function [59]). This is consistent with recent work [50] that reported the stretched exponential decay of real time correlation functions. The fitting procedure [51] results in E_{Th} shown in Fig. 3(d). The exponent β , which controls the asymptotic power-law behavior of the spectral function is illustrated in Fig. 3(e). The spectral function $f^2(\omega)$ behaves as $1/\omega^{1+\beta}$ for $\omega \gg E_{\text{Th}}$.

We note that β exhibits non-monotonic behavior with maximum around the transition point. In addition, in vicinity of transition, we observe a collapse of spectral function $f^2(\omega)/2^L$ plotted as a function of $\omega/\delta_{\text{av}}$ for different system sizes, see [51].

Discussion.— We have studied and compared the behavior of E_{Th} across the Floquet many-body localization transition obtained using various probes based on spectral properties and matrix elements of local observables. Among the considered probes, SFF and spectral function work well on the ergodic side yielding consistent values of E_{Th} that saturates at a value independent of system size. This is in contrast to the Hamiltonian models, where $E_{\text{Th}}(L) \propto L^{-1/\gamma}$ exhibits subdiffusive scaling with L with a disorder-dependent exponent [60]. In the critical region, E_{Th} becomes of the order of many-body level spacing. In the critical region the extraction of E_{Th} from the SFF and spectral function becomes unreliable, and we obtain E_{Th} from the most probable value of the level spacing and many-body Thouless parameter.

In addition to scrutinizing different notions of E_{Th} , our work provides new insights into the MBL transition in the Floquet model. The absence of any conserved quantities in the considered model reduces the finite size effects, which is manifested in the larger value of the critical exponent and weaker drift of the critical point, in agreement with earlier numerical studies of a different model using a different set of probes [15]. Moreover, we find the properties of spectral functions to be consistent with the

stretched exponential relaxation of real-time correlation functions [50].

Several open questions remain for future work. In particular, in light of an apparent absence of subdiffusion in the ergodic phase in Floquet models, it would be interesting to investigate the rare-region effects on the spreading of entanglement, correlation functions decay, and implications for the nature of the transition into the MBL phase. Furthermore, the link between different definitions of E_{Th} established here may serve as a foundation for developing a scaling theory of the Floquet-MBL transition.

Note added.— While this paper was being finalized, Ref. [61] appeared which investigates SFF in a Floquet model of MBL using dual disorder-averaged transfer matrix approach also employed above.

Acknowledgements.— This work was supported by the Swiss National Science Foundation (Mi.So. and D.A.), and by the European Research Council (ERC) under the European Union’s Horizon 2020 research and innovation programme (Ma.Se., grant agreement No. 850899, and D.A., grant agreement No. 864597). Z.P. acknowledges support by EPSRC grant EP/R020612/1 and by the Leverhulme Trust Research Leadership Award RL-2019-015. Statement of compliance with EPSRC policy framework on research data: This publication is theoretical work that does not require supporting research data. The computations were performed on the Baobab cluster of the University of Geneva.

-
- [1] E. Altman and R. Vosk, “Universal dynamics and renormalization in many body localized systems,” ArXiv e-prints (2014), [arXiv:1408.2834 \[cond-mat.dis-nn\]](#).
 - [2] Rahul Nandkishore and David A. Huse, “Many-body localization and thermalization in quantum statistical mechanics,” *Annual Review of Condensed Matter Physics* **6**, 15–38 (2015).
 - [3] Dmitry A. Abanin, Ehud Altman, Immanuel Bloch, and Maksym Serbyn, “Colloquium: Many-body localization, thermalization, and entanglement,” *Rev. Mod. Phys.* **91**, 021001 (2019).
 - [4] Fabien Alet and Nicolas Laflorencie, “Many-body localization: An introduction and selected topics,” *Comptes Rendus Physique* **19**, 498 – 525 (2018), quantum simulation / Simulation quantique.
 - [5] M. Znidaric, T. Prosen, and P. Prelovsek, “Many-body localization in the Heisenberg XXZ magnet in a random field,” *Phys. Rev. B* **77**, 064426 (2008).
 - [6] Jens H. Bardarson, Frank Pollmann, and Joel E. Moore, “Unbounded growth of entanglement in models of many-body localization,” *Phys. Rev. Lett.* **109**, 017202 (2012).
 - [7] Maksym Serbyn, Z. Papić, and Dmitry A. Abanin, “Local conservation laws and the structure of the many-body localized states,” *Phys. Rev. Lett.* **111**, 127201 (2013).
 - [8] David A. Huse, Rahul Nandkishore, and Vadim Oganesyan, “Phenomenology of fully many-body-localized systems,” *Phys. Rev. B* **90**, 174202 (2014).
 - [9] J. M. Deutsch, “Quantum statistical mechanics in a closed system,” *Phys. Rev. A* **43**, 2046–2049 (1991).
 - [10] Mark Srednicki, “Chaos and quantum thermalization,” *Phys. Rev. E* **50**, 888–901 (1994).
 - [11] Marcos Rigol, Vanja Dunjko, and Maxim Olshanii, “Thermalization and its mechanism for generic isolated quantum systems,” *Nature* **452**, 854–858 (2008).
 - [12] Achilleas Lazarides, Arnab Das, and Roderich Moessner, “Fate of many-body localization under periodic driving,” *Phys. Rev. Lett.* **115**, 030402 (2015).
 - [13] Pedro Ponte, Z. Papić, François Huveneers, and Dmitry A. Abanin, “Many-body localization in periodically driven systems,” *Phys. Rev. Lett.* **114**, 140401 (2015).
 - [14] Dmitry A. Abanin, Wojciech De Roeck, and François Huveneers, “Theory of many-body localization in periodically driven systems,” *Annals of Physics* **372**, 1 – 11 (2016).
 - [15] Liangsheng Zhang, Vedika Khemani, and David A. Huse, “A floquet model for the many-body localization transition,” *Phys. Rev. B* **94**, 224202 (2016).
 - [16] Christoph Sündershauf, David Pérez-García, David A. Huse, Norbert Schuch, and J. Ignacio Cirac, “Localization with random time-periodic quantum circuits,” *Phys. Rev. B* **98**, 134204 (2018).
 - [17] Talía L. M. Lezama, Soumya Bera, and Jens H. Bardarson, “Apparent slow dynamics in the ergodic phase of a driven many-body localized system without extensive conserved quantities,” *Physical Review B* **99**, 161106 (2019).

- (2019), publisher: American Physical Society.
- [18] Vedika Khemani, Achilleas Lazarides, Roderich Moessner, and S. L. Sondhi, “Phase structure of driven quantum systems,” *Phys. Rev. Lett.* **116**, 250401 (2016).
 - [19] Dominic V. Else, Bela Bauer, and Chetan Nayak, “Floquet time crystals,” *Phys. Rev. Lett.* **117**, 090402 (2016).
 - [20] Hoi Chun Po, Lukasz Fidkowski, Takahiro Morimoto, Andrew C. Potter, and Ashvin Vishwanath, “Chiral Floquet phases of many-body localized bosons,” *Phys. Rev. X* **6**, 041070 (2016).
 - [21] Frederik Nathan, Dmitry Abanin, Erez Berg, Netanel H. Lindner, and Mark S. Rudner, “Anomalous floquet insulators,” *Phys. Rev. B* **99**, 195133 (2019).
 - [22] Soonwon Choi, Joonhee Choi, Renate Landig, Georg Kucsko, Hengyun Zhou, Junichi Isoya, Fedor Jelezko, Shinobu Onoda, Hitoshi Sumiya, Vedika Khemani, Curt von Keyserlingk, Norman Y. Yao, Eugene Demler, and Mikhail D. Lukin, “Observation of discrete time-crystalline order in a disordered dipolar many-body system,” *Nature* **543**, 221–225 (2017).
 - [23] Joonhee Choi, Hengyun Zhou, Soonwon Choi, Renate Landig, Wen Wei Ho, Junichi Isoya, Fedor Jelezko, Shinobu Onoda, Hitoshi Sumiya, Dmitry A. Abanin, and Mikhail D. Lukin, “Probing quantum thermalization of a disordered dipolar spin ensemble with discrete time-crystalline order,” *Phys. Rev. Lett.* **122**, 043603 (2019).
 - [24] Pranjal Bordia, Henrik Lüschen, Ulrich Schneider, Michael Knap, and Immanuel Bloch, “Periodically driving a many-body localized quantum system,” *Nature Physics* **13**, 460–464 (2017).
 - [25] J. Zhang, P. W. Hess, A. Kyprianidis, P. Becker, A. Lee, J. Smith, G. Pagano, I. D. Potirniche, A. C. Potter, A. Vishwanath, N. Y. Yao, and C. Monroe, “Observation of a discrete time crystal,” *Nature* **543**, 217–220 (2017).
 - [26] B. Kramer and A. MacKinnon, “Localization: theory and experiment,” *Reports on Progress in Physics* **56**, 1469–1564 (1993), publisher: IOP Publishing.
 - [27] F. Evers and A. D. Mirlin, “Anderson Transitions,” *Reviews of Modern Physics* **80**, 1355–1417 (2008), arXiv: 0707.4378.
 - [28] J T Edwards and D J Thouless, “Numerical studies of localization in disordered systems,” *Journal of Physics C: Solid State Physics* **5**, 807 (1972).
 - [29] E. Abrahams, P. W. Anderson, D. C. Licciardello, and T. V. Ramakrishnan, “Scaling theory of localization: Absence of quantum diffusion in two dimensions,” *Phys. Rev. Lett.* **42**, 673–676 (1979).
 - [30] Maksym Serbyn, Z. Papić, and Dmitry A. Abanin, “Criterion for many-body localization-delocalization phase transition,” *Phys. Rev. X* **5**, 041047 (2015).
 - [31] Corentin L. Bertrand and Antonio M. García-García, “Anomalous thouless energy and critical statistics on the metallic side of the many-body localization transition,” *Phys. Rev. B* **94**, 144201 (2016).
 - [32] Amos Chan, Andrea De Luca, and J. T. Chalker, “Spectral statistics in spatially extended chaotic quantum many-body systems,” *Phys. Rev. Lett.* **121**, 060601 (2018).
 - [33] Abhishodh Prakash, J. H. Pixley, and Manas Kulkarni, “The universal spectral form factor for many-body localization,” arXiv e-prints, arXiv:2008.07547 (2020), arXiv:2008.07547 [cond-mat.dis-nn].
 - [34] Piotr Sierant, Dominique Delande, and Jakub Zakrzewski, “Thouless Time Analysis of Anderson and Many-Body Localization Transitions,” *Physical Review Letters* **124**, 186601 (2020).
 - [35] Michele Filippone, Piet W. Brouwer, Jens Eisert, and Felix von Oppen, “Drude weight fluctuations in many-body localized systems,” *Phys. Rev. B* **94**, 201112 (2016).
 - [36] Céile Monthus, “Many-body-localization transition: sensitivity to twisted boundary conditions,” *Journal of Physics A: Mathematical and Theoretical* **50**, 095002 (2017).
 - [37] Maksym Serbyn, Z. Papić, and Dmitry A. Abanin, “Thouless energy and multifractality across the many-body localization transition,” *Phys. Rev. B* **96**, 104201 (2017).
 - [38] Mauro Schiulaz, E. Jonathan Torres-Herrera, and Lea F. Santos, “Thouless and relaxation time scales in many-body quantum systems,” *Physical Review B* **99**, 174313 (2019), publisher: American Physical Society.
 - [39] Ronen Vosk, David A. Huse, and Ehud Altman, “Theory of the many-body localization transition in one-dimensional systems,” *Phys. Rev. X* **5**, 031032 (2015).
 - [40] Andrew C. Potter, Romain Vasseur, and S. A. Parameswaran, “Universal properties of many-body delocalization transitions,” *Phys. Rev. X* **5**, 031033 (2015).
 - [41] D. A. Abanin, J. H. Bardarson, G. De Tomasi, S. Gopalakrishnan, V. Khemani, S. A. Parameswaran, F. Pollmann, A. C. Potter, M. Serbyn, and R. Vasseur, “Distinguishing localization from chaos: challenges in finite-size systems,” arXiv e-prints, arXiv:1911.04501 (2019), arXiv:1911.04501 [cond-mat.str-el].
 - [42] Arijeet Pal and David A. Huse, “Many-body localization phase transition,” *Phys. Rev. B* **82**, 174411 (2010).
 - [43] Madan Lal Mehta, *Random matrices* (Elsevier, 2004).
 - [44] David J. Luitz, Nicolas Laflorencie, and Fabien Alet, “Many-body localization edge in the random-field Heisenberg chain,” *Phys. Rev. B* **91**, 081103 (2015).
 - [45] W. de Roeck, F. Huveneers, M. Müller, and M. Schiulaz, “Absence of many-body mobility edges,” ArXiv e-prints (2015), arXiv:1506.01505 [cond-mat.dis-nn].
 - [46] M Akila, D Waltner, B Gutkin, and T Guhr, “Particle-time duality in the kicked ising spin chain,” *Journal of Physics A: Mathematical and Theoretical* **49**, 375101 (2016).
 - [47] Michael Sonner, Alessio Lerose, and Dmitry A. Abanin, “Characterizing many-body localization via exact disorder-averaged quantum noise,” (2020), arXiv:2012.00777 [cond-mat.dis-nn].
 - [48] Bruno Bertini, Pavel Kos, and Tomaz Prosen, “Exact spectral form factor in a minimal model of many-body quantum chaos,” *Phys. Rev. Lett.* **121**, 264101 (2018).
 - [49] Alessio Lerose, Michael Sonner, and Dmitry A. Abanin, “Influence matrix approach to many-body Floquet dynamics,” arXiv:2009.10105 [cond-mat, physics:quant-ph] (2020), arXiv: 2009.10105.
 - [50] Talía L. M. Lezama, Soumya Bera, and Jens H. Bardarson, “Apparent slow dynamics in the ergodic phase of a driven many-body localized system without extensive conserved quantities,” *Phys. Rev. B* **99**, 161106 (2019).
 - [51] Supplemental online material.
 - [52] Fritz Haake, *Quantum Signatures of Chaos* (Springer-Verlag, Berlin, Heidelberg, 2006).
 - [53] Vadim Oganesyan and David A. Huse, “Localization of interacting fermions at high temperature,” *Phys. Rev. B* **75**, 155111 (2007).

- [54] Luca D'Alessio and Marcos Rigol, "Long-time behavior of isolated periodically driven interacting lattice systems," [Phys. Rev. X **4**, 041048 \(2014\)](#).
- [55] E. Brézin and S. Hikami, "Spectral form factor in a random matrix theory," [Phys. Rev. E **55**, 4067–4083 \(1997\)](#).
- [56] David J. Luitz and Yevgeny Bar Lev, "Anomalous thermalization in ergodic systems," [Phys. Rev. Lett. **117**, 170404 \(2016\)](#).
- [57] A Brooks Harris, "Effect of random defects on the critical behaviour of ising models," *Journal of Physics C: Solid State Physics* **7**, 1671 (1974).
- [58] A. Chandran, C. R. Laumann, and V. Oganesyan, "Finite size scaling bounds on many-body localized phase transitions," *ArXiv e-prints* (2015), [arXiv:1509.04285 \[cond-mat.dis-nn\]](#).
- [59] Joachim Wuttke, "Laplace-Fourier transform of the stretched exponential function: Analytic error bounds, double exponential transform, and open-source implementation libkww" [Algorithms **5**, 604–628 \(2012\)](#).
- [60] Kartiek Agarwal, Ehud Altman, Eugene Demler, Sarang Gopalakrishnan, David A. Huse, and Michael Knap, "Rare-region effects and dynamics near the many-body localization transition," [Annalen der Physik **529**, 1600326 \(2017\)](#).
- [61] S. J. Garratt and J. T. Chalker, "Many-body delocalisation as symmetry breaking," *arXiv e-prints*, [arXiv:2012.11580](#) (2020), [arXiv:2012.11580 \[cond-mat.stat-mech\]](#).